Stochastic resonance and the dithering effect in threshold physical systems

Luca Gammaitoni*
Istituto Nazionale di Fisica Nucleare, Sezione di Perugia, and Dipartimento di Fisica, Università di Perugia, I-06100 Perugia, Italy
(Received 4 May 1995; revised manuscript received 18 August 1995)

There is a wide class of phenomena which can be interpreted by using a dynamical system with a threshold as a model. Examples of these systems can be found in fields as diverse as digital communication and neurobiology. In this paper we discuss the dynamical behavior of threshold systems in the presence of noise. We show that both the dithering effect, well known to electronic engineers since the 1950s, and the phenomenon of stochastic resonance in threshold systems, recently introduced in the physical literature, can be described within the same scheme of noise activated processes. For these phenomena, in the absence of any frequency matching condition, the use of the term resonance is questionable and the notion of noise induced threshold crossings is more appropriate.

PACS number(s): 05.40.+j, 02.50.−r

I. INTRODUCTION

Dynamical models which make use of threshold devices have been employed, in recent years, in many fields of scientific research to describe a wide range of physical phenomena. Examples of these systems can be found in fields as diverse as digital communication (e.g., analog to digital conversion), neurobiology (e.g., neuron firing), natural events (e.g., avalanches), laser systems (e.g., laser threshold), complex systems (e.g., bifurcations), chemical systems (e.g., activation threshold), and political sciences (e.g., electoral schemes). Typically, nothing happens in these systems as long as a certain control parameter remains below a threshold value. As soon as the control parameter exceeds the threshold value, everything that happens does so (almost) instantaneously.

As an example let us consider the following simple threshold system in which y is the output of a system S to the input x:

$$y = \begin{cases} 0 & \text{for } x < \frac{1}{2} \\ 1 & \text{for } x > \frac{1}{2}. \end{cases} \tag{1}$$

Here the threshold value has been set equal to 1/2 and $0 \leq x \leq 1$. We can represent the action of system S, in short form, as $y = Q[x]$. The response characteristic of S is illustrated in Fig. 1(a) (see Sec. II). For comparison, a linear response characteristic is also shown. The linear response output consists of a slowly changing ramp $y = x$ going from one level (state 0) to the next (state 1) continuously. Instead, the threshold system output $y = Q[x]$, corresponding to a quantized signal, switches in one step from 0 to 1 when x crosses the threshold value. Here, this value has been placed at half the step magnitude but, in general, x and y can have different domains.

Threshold systems can also be seen as a basic model for the wider class of bistable dynamical systems. In

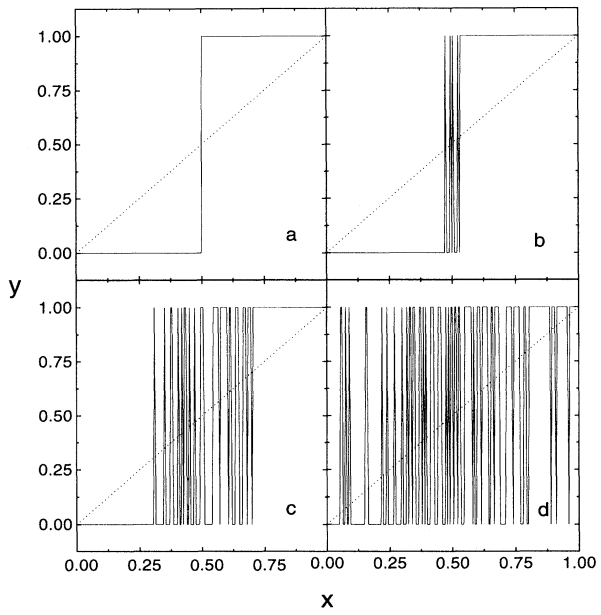

FIG. 1. Threshold system output y vs x (solid line): (a) in the absence of noise dither [for comparison we report also the linear response characteristic $y = x$ (dotted line)]; (b) y with dither noise of intensity $L = 0.1$; (c) $L = 0.5$; and (d) $L = 1.0$. The data presented in this paper have been obtained via digital simulation. Noise intensity, system input and output are expressed here in arbitrary units (a.u.).

*Electronic address: Gammaitoni @perugia.infn.it

these systems some of the peculiar phenomena observed in the presence of bistability still survive. Among these the stochastic resonance phenomenon (SR) [1,2] recently gained some popularity. The SR was proposed more than ten years ago as a possible nonlinear mechanism to enhance the effect of a small periodic force by adding to it some external noise of a proper intensity. It was experimentally observed [2] in a number of bistable physical systems. Recently some attention has been devoted to the study of SR in threshold systems [3–6], with the aim being to realize signal processing oriented devices [6] operating under the SR condition.

The effect of adding noise to the input signal on the response characteristic of a threshold system is the subject of the present paper, which is organized as follows.

In Sec. II, we start discussing a well known noise induced phenomenon in threshold systems: the dithering effect. In digital signal processing [7], an analog signal is sampled at discrete times and converted into a sequence of numbers. Since the register length is finite, the conversion procedure, called signal quantization, results in distortion and a loss of signal detail. In order to avoid distortion and recover signal detail, it has become a common practice, since the 1950s, to add a small amount of noise to the analog signal before quantization — a technique called dithering. In this section we briefly review the dithering effect as developed in the digital signal processing theory and propose a detailed description of the optimal condition for the linearity of the response characteristic.

The noise-induced threshold crossing, within the framework of the stochastic resonance phenomenon, is the subject of Sec. III. There, we show that, for the class of threshold systems considered here, there is no frequency dependence in the system response, and the increase in the periodic output amplitude can be explained without recourse to any synchronization condition, as a special case of the dithering effect discussed in Sec. II.

In Sec. IV we conclude with a short comment on the relation between dithering as a noise-induced threshold crossing effect, and stochastic resonance as a frequency matching condition.

II. THE DITHERING EFFECT

Digital signal processing is a widespread and powerful collection of techniques in signal analysis [7] that is commonly used in many fields of scientific research and human activity. When applied to the physical sciences, the digital sequence to be processed is generally obtained by sampling a band limited physical signal at discrete intervals of time. The sequence of samples thus obtained is usually stored, in a binary format, in finite word length registers. Conversion from a continuous (analog) signal to a digital one consists of two different operations: time discretization and amplitude quantization. Time discretization, if properly applied, can be shown to be error free. The effects of amplitude quantization (finite word-length) are instead always present and manifest themselves in a number of different ways. First, due to the presence of a nonlinear response characteristic, signal quantization leads to an unavoidable distortion, i.e., the presence of spurious signals in a frequency band different from the original one. There is also a loss of signal detail that is small compared to the quantization step (the dynamic range of a digital signal is finite). In the following, we will refer to the simple and more common case of uniform rounding quantization [as in Eq. (1)].

To deal with such effects, engineers have developed a general scheme [8–16] in which the notion of quantization error, η, plays a central role. $\eta = y - x$ represents the *error* introduced by the coarseness of the amplitude quantization in the analog-to-digital conversion. It is clear from this definition that if we had a linear response characteristic (apart from amplification factors), η would be zero. Usually η is treated as an additive noise whose statistical properties depend upon the input signal x [8,9]. It has been shown [10,11], however, that the minimum loss of statistical data from the input x occurs when the quantization error can be made independent of x. In the search for a technique to realize such an independence condition, it was proposed to use an added external signal (dither) before quantization. A number of studies on the proper choices of dither signals were performed in the last 30 years [8–16]. The main conclusions can be summarized as follows: (i) the addition of a proper dither signal can cause the independence and whitening of the quantization error resulting in both a reduction of signal distortion and an improvement of the system dynamic range; (ii) the best choice for the dither signal is a random dither uniformly distributed within an interval of amplitude equal to the quantization step.

In this paper we propose a different approach to the study of the dithering effect. Instead of considering the statistics of the quantization noise η, which depends on the input signal x, we focus on the statistics of the dither signal. Let us start by considering the system S introduced before. In Fig. 1(b), a sample output y to a ramp x with a small uniform noise added to it is shown. The presence of the noise induces random jumps concentrated in a small interval (jump region) centered around the threshold value $x = 0.5$. When one increases the noise intensity, the jump region extends symmetrically [Fig. 1(c)] up to cover the whole input interval [Fig. 1(d)]. Figure 2 reproduces the average output $\langle y_u \rangle$, for different noise values. As can be seen, the averaged system response characteristic is a function of the noise and approaches the linear one as the noise intensity approaches the quantization step. Figure 3 reproduces the averaged output $\langle y_g \rangle$ in the presence of a white Gaussian noise. In this case, the averaged output $\langle y_g \rangle$ differs qualitatively from the uniform noise case. In order to quantitatively compare the averaged system response characteristic in the presence of either uniform or Gaussian noise with the linear response, we introduce the quantity D:

$$D = \sqrt{\int_0^1 (\langle y \rangle - x)^2 dx} \ . \tag{2}$$

D is a measure of the distance between $\langle y \rangle$ and the linear response $y = x$. In Fig. 4, we plot D *versus* σ

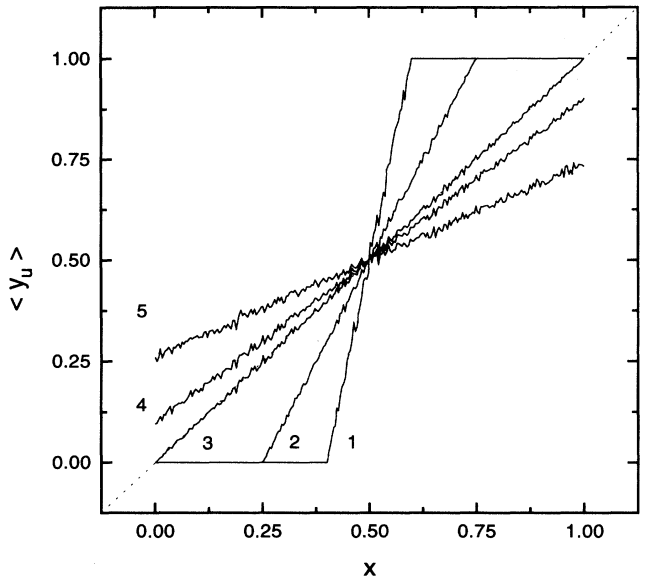

FIG. 2. Averaged system output $\langle y_u \rangle$ vs x for various uniform noise intensities: (1) $L = 0.2$; (2) $L = 0.5$; (3) $L = 1.0$; (4) $L = 1.25$; (5) $L = 2.1$. For comparison we report also the linear response characteristic (dotted line). All the quantities are in a.u..

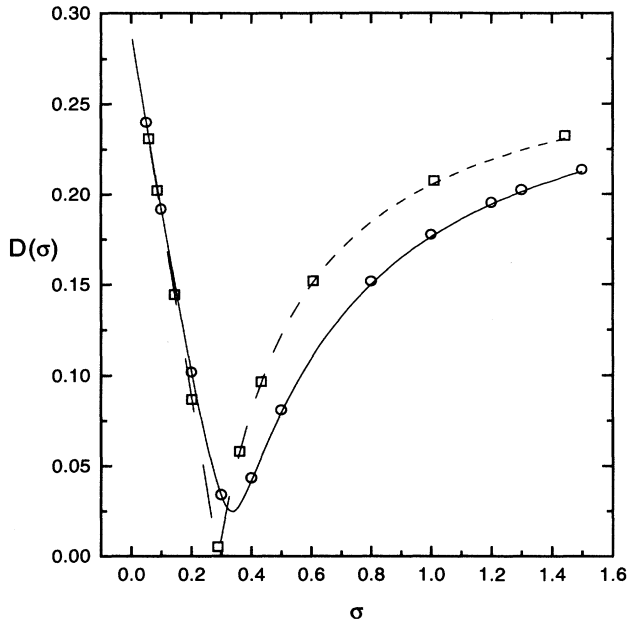

FIG. 4. D (a.u.) vs σ (a.u.). Gaussian noise: digital simulation (circles), theory (solid line). Uniform noise: digital simulation (squares), theory (dashed line). Statistical errors are within 3%.

for both uniform and Gaussian noise [17]. In the small noise region, the two curves are almost the same. As the noise intensity increases, however, a qualitative difference becomes apparent; in the uniform noise case, D reaches the value $D = 0$, which means that the averaged output $\langle y \rangle$ coincides with the linear characteristic

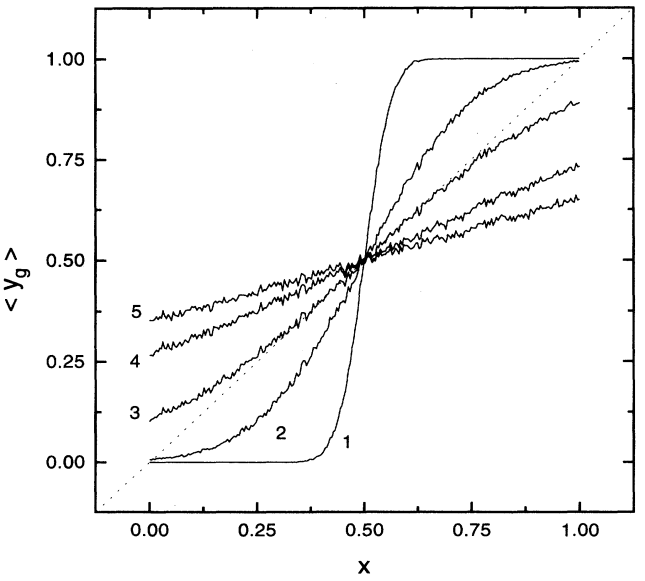

FIG. 3. Averaged system output $\langle y_g \rangle$ vs x for various Gaussian noise intensities: (1) $\sigma = 0.05$; (2) $\sigma = 0.2$; (3) $\sigma = 0.4$; (4) $\sigma = 0.8$; (5) $\sigma = 1.3$. For comparison we report also the linear response characteristic (dotted line). All the quantities are in a.u.

x. Such an optimal condition is not reached in the case of Gaussian noise, where D remains greater than zero for all the noise values. It is worth noticing that the minimum value $D = 0$ is reached, in the uniform noise case, when the standard deviation $\sigma = 1/\sqrt{12}$. This amounts to a uniform noise with amplitude $L = 1$ equal to the quantization step, as previously stated in (ii). For larger noise intensity, the Gaussian case crosses the uniform one and remains smaller for all the noise values. The distance between the two curves decreases for larger noise intensity. In both cases, the D vs σ shows a nonmonotonic behavior with a clear minimum. This means that an optimal noise value exists where the averaged output response characteristic comes closer to the linear one. In particular, for the uniform noise case, if the intensity of the noise is properly matched, the averaged output is indistinguishable from the linear response output. Such a noise induced linearization is a phenomenon which has been already observed in a number of cases for a variety of nonlinear systems [18].

Here, we propose a theoretical description for the case of threshold systems. The D versus σ evolution can be described by considering the probability density function (PDF) $f(\xi)$ of the noise dither added to the input signal (we use the notation with subscripts u and g, as in ξ_u and ξ_g, to distinguish between the uniform and Gaussian case, respectively). The average value of the system response can be written as

$$\langle y \rangle = \langle Q[x + \xi] \rangle = \int_{-\infty}^{+\infty} Q[x + \xi] f(\xi) d\xi \ . \qquad (3)$$

This integral can be rewritten in terms of the *distribution function* $F(z)$:

$$F[z] = \int_{-\infty}^{z} f(\xi)d\xi$$

as

$$\langle y \rangle = \int_{\frac{1}{2}-x}^{+\infty} f(\xi)d\xi = 1 - F\left[\frac{1}{2} - x\right] . \quad (4)$$

The integration interval in (3) has been reduced here to the noise values which satisfy the condition $x + \xi > 1/2$, due to the action of the operator $Q[x + \xi]$. We note that $\langle y \rangle$ is a function of x and σ and coincides with the transition probability of the process $x + \xi$.

For the uniform noise case, (4) becomes

$$\langle y_u \rangle = \begin{cases} 0 & \text{for } x < \frac{1}{2} - \frac{L}{2} \text{ or } x > \frac{1}{2} + \frac{L}{2} \\ \frac{1}{L}(x + \frac{L}{2} - \frac{1}{2}) & \text{for } \frac{1}{2} - \frac{L}{2} \le x \le \frac{1}{2} + \frac{L}{2} , \end{cases} \quad (5)$$

where the PDF has been defined as

$$f_u(\xi) = \frac{1}{L} \text{ for } -\frac{L}{2} \le \xi_u \le \frac{L}{2} \quad (6)$$

and zero elsewhere. For the Gaussian noise case, (4) becomes

$$\langle y_g \rangle = \frac{1}{2} - \Phi\left[\frac{(\frac{1}{2} - x)}{\sigma}\right] , \quad (7)$$

where

$$\Phi\left[\frac{z}{\sigma}\right] = \frac{1}{\sigma\sqrt{2\pi}} \int_0^z e^{\frac{-t^2}{2\sigma^2}} dt$$

is the error function. We are now in a position to calculate the curves, D vs σ, for the two noise cases considered above. Theoretical predictions shown in Fig. 4 are in very good agreement with the digital simulations.

We note that as long as we are concerned with distortion, the optimal dither signal consists of a uniform noise with amplitude equal to the quantization step. In this case, the averaged quantization error is zero. For smaller noise values, clipping effects on the signal are present while for larger noise values, a reduction of the system output range affects the response. In both cases, the quantization error does not average to zero. Gaussian noise, although showing qualitatively similar positive effects, is characterized by a worse performance.

It is worth noticing that the addition of noise plus averaging procedure plays a crucial role in both the linearizing mechanism and the increase of dynamic range. As an example, let us consider a constant input signal which has an amplitude of 0.2 (threshold at 0.5). To achieve a correct representation of this signal at the output, we should arrange the system in order to have an averaged output of 0.2. This result can be obtained if the signal crosses the threshold two times out of ten (on average). In such a case, we collect two "1"'s and eight "0"'s which, averaged, make 0.2. To reach linearity such a probability should be kept equal for all the input range, i.e., we need a dither signal which is uniform over the whole quantization step and has an amplitude equal to the quantization step itself. The problem with Gaussian noise is that the PDF is not uniform. With such a noise source, the better performance, with respect to distortion, is reached in the x range where the PDF is more uniform, i.e., around the origin or, for a fixed x interval, when $\sigma \to \infty$. However in that case the output range is dramatically reduced.

The simple case analyzed before also serves to shed some light on the subject of increase in dynamic range due to the presence of dithering [14]. In the absence of dithering, we have just one bit, no matter how we average. For this reason, the signal of amplitude 0.2 will be read as just "0." As we saw before, with an optimal dither and averaging at least ten times, we can increase the dynamic range enough to distinguish a signal of amplitude 0.2. It seems evident that if we want to increase the dynamic range enough to distinguish a signal of amplitude 0.22, we need at least ten times as many averages (see, e.g., oversampling techniques [19], implemented in modern analog-to-digital converter systems). From what we have said, it is clear that the averaging procedure is truly efficient in increasing the dynamic range only if the dither signal can span the entire input range with constant probability. This is again the same condition met before for an absence of distortion. We do not address this issue any further in this paper.

III. STOCHASTIC RESONANCE IN THRESHOLD SYSTEMS

In this section, we will show that SR, as observed in threshold devices, can be interpreted under the same scheme as the dithering effect. In fact, the dithering effect shows an optimal condition that can be achieved by tuning the noise intensity, just like the SR condition. Moreover, in this case, for the SR condition the frequency of the periodic input does not play any role. The evidence of SR in multithreshold systems will be given as well.

Let us consider a harmonic signal $x(t) = A\sin(\omega_0 t)$ [20] at the input of a threshold system. To take into account the symmetrical shape of the signal x, we slightly modify our previous system S according to the following rule:

$$y(t) = \begin{cases} -1 & \text{for } x < -\frac{1}{2} \\ 0 & \text{for } -\frac{1}{2} < x < \frac{1}{2} \\ 1 & \text{for } x > \frac{1}{2} . \end{cases} \quad (8)$$

In this system, there are two symmetrical thresholds, centered around zero. Zero is also the average value of the input signal and of the additive (dither) noise. The amplitude A is chosen smaller than the threshold value so that, in the absence of noise, the system output y is always equal to zero. The addition of noise induces random jumps above the upper and beyond the lower threshold causing y to switch from "0" to "1" or "−1." We are interested in monitoring the presence of the input signal x in the output y. For this reason we consider the $y(t)$ time series and compute the corresponding power

spectral density $S_y(\omega)$. The statistical weight of the periodic component in the output signal can be monitored by measuring the height of the narrow peak in $S_y(\omega)$ at $\omega = \omega_0$. To eliminate the effect of random jumps, we subtract the continuous background $N(\omega_0)$ and define $P_y = \sqrt{S_y(\omega_0) - N(\omega_0)}$.

The behavior of $P_y = P_y(\sigma)$ for three different values of amplitude A, for both the white Gaussian noise and white uniform noise cases, is shown in Fig. 5. As can be seen, $P_y(\sigma)$ shows the typical SR profile: a sharp increase up to a maximum value (resonant condition) and a slow decrease. Apart from these features, common to both cases, some differences are apparent. The uniform noise curve is generally sharper and more pronounced, the maxima happen at slightly different noise values. For large noise, the Gaussian dither performs better than the uniform one. The difference between the two curves decreases with increasing σ and A.

A quantitative description of the $P_y(\sigma)$ behavior can be given following the reasoning already introduced in Sec. II. In order to have a large periodic component at the threshold system output y, the action of the added noise should produce upward jumps (and inhibit downward jumps) in coincidence with the half period in which $x(t) > 0$. The same requirement holds for the symmetrical situation of the downward jumps in the half period in which $x(t) < 0$. This condition can be restated in terms of the threshold crossing probability, as in Sec. II. If we generically call $b/2$ the distance between the "0" level and the threshold (in Sec. II $b = 1$ was equal to the quantization step), we can introduce the quantity

$$A_y(\sigma) = F\left[\frac{b}{2} + A\right] - F\left[\frac{b}{2} - A\right] . \tag{9}$$

$A_y(\sigma)$ is a measure of the probability that y jumps from state "0" to state "1" when $x > 0$ *and* does not when $x < 0$. We can interpret $A_y(\sigma)$ as proportional to the amplitude of the periodic component of the output $y(t)$, at the input frequency $\nu_0 = \omega_0/2\pi$, $A_y(\sigma) = kP_y(\sigma)$. In spite of the simplicity of the assumptions made [we ignored the periodic character and the actual shape of the input function $x(t)$], $A_y(\sigma)$ reproduces fairly well (Fig. 5) the behavior of $P_y(\sigma)$, for a wide range of noise intensities σ and forcing amplitudes A, both for the Gaussian

$$A_{yg}(\sigma) = k\left(\Phi\left[\frac{\left(\frac{b}{2} + A\right)}{\sigma}\right] - \Phi\left[\frac{\left(\frac{b}{2} - A\right)}{\sigma}\right]\right) \tag{10}$$

and for the uniform noise case

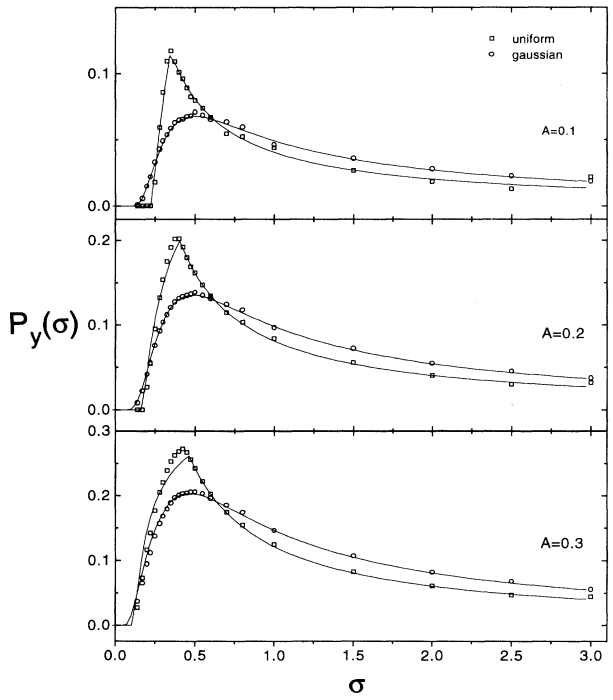

FIG. 5. P_y (a.u.) vs σ (a.u.) for Gaussian noise (circles) and uniform noise (squares), for three different values of the input amplitude A: upper $A = 0.1$, middle $A = 0.2$, lower $A = 0.3$, in a.u.. Theoretical predictions A_y are shown with solid lines, $k = 0.7$. Statistical errors are within 10%.

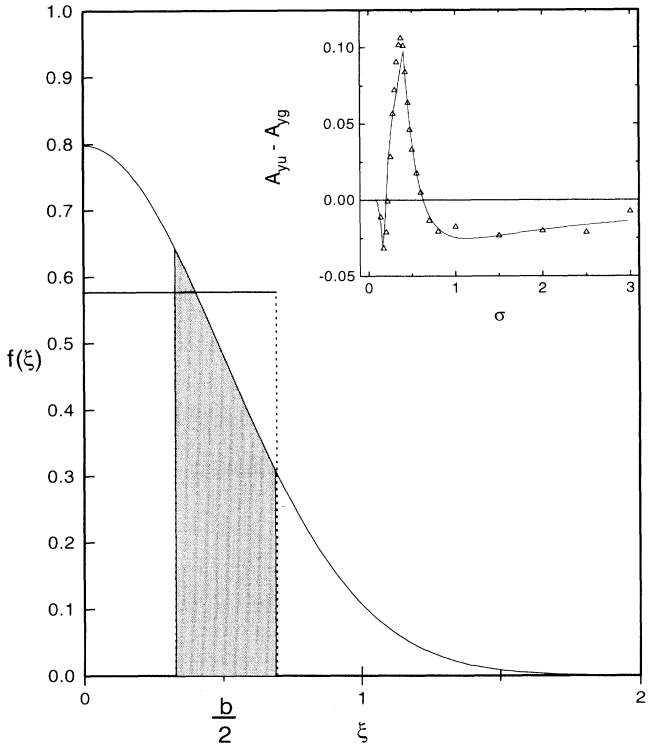

FIG. 6. $f(\xi)$ (a.u.) for Gaussian and uniform noise. The area under the distributions and enclosed between $b/2 - A$ and $b/2 + A$ (dotted lines) equals A_{yu} and A_{yg} (shaded area), $\sigma_g = \sigma_u = 1$ (a.u.). Inset: $A_{yu} - A_{yg}$ vs σ, $A = 0.2$ (a.u.), theroretical prediction (solid line), and experimental data $P_{yu} - P_{yg}$ (triangles).

$$A_{yu}(L) = k \begin{cases} 0 & \text{for } \frac{L}{2} < \frac{b}{2} - A \\ \frac{1}{L}\left(\frac{L}{2} - \frac{b}{2} + A\right) & \text{for } \frac{b}{2} - A \le \frac{L}{2} \le \frac{b}{2} + A \\ \frac{2A}{L} & \text{for } \frac{L}{2} > \frac{b}{2} + A \end{cases} \tag{11}$$

with k constant related to the bin amplitude of the digitally simulated PSD. As we anticipated, the positions of the two maxima do not coincide. In the Gaussian case, the maximum for A_{yg} occurs at

$$\sigma_g = \sqrt{\frac{bA}{ln\left(\frac{b+2A}{b-2A}\right)}} \approx \frac{b}{2} - \frac{A^2}{3b} + O(A^4) , \tag{12}$$

while for the uniform noise case, the maximum occurs at

$$\sigma_u = \frac{1}{\sqrt{3}}\left(\frac{b}{2} + A\right) \text{ or } \frac{L}{2} = \left(\frac{b}{2} + A\right) . \tag{13}$$

Most notably σ_u increases with A while σ_g decreases. They coincide for $A \approx 0.3$ (see Fig. 5). Figure 6 offers a pictorial representation of the quantity A_y, meant as the area under the PDF, between $b/2 - A$ and $b/2 + A$ (area delimited by the dotted lines in Fig. 6). It is apparent that the area under the Gaussian PDF (shaded area) is smaller than the area under the uniform PDF until about $\sigma \le b/2$. For $\sigma \to \infty$ the two regions become asymptotically equal and the difference between A_{yg} and A_{yu} tends to disappear (inset of Fig. 6).

A. Specialized noise dither

Following this reasoning, the performance of our threshold device can be increased by introducing a proper noise dither which maximizes the shaded area. Such a noise has a disjoint uniform PDF, half centered around the threshold value $b/2$ and half centered around $-b/2$:

$$f_d(\xi) = \frac{1}{2L} \text{ for } \pm\frac{b}{2} - \frac{L}{2} \le \xi_u \le \pm\frac{b}{2} + \frac{L}{2} \tag{14}$$

and zero elsewhere. The amplitude $A_y(\sigma)$, for this case, is easily computed to be

$$A_{yd}(L) = k \begin{cases} \frac{A}{L} & \text{for } A < \frac{L}{2} < b - A \\ \frac{A}{L} + \frac{1}{2L}\left(\frac{L}{2} - b + A\right) & \text{for } b - A < \frac{L}{2} < b + A \\ \frac{2A}{L} & \text{for } \frac{L}{2} > b + A , \end{cases} \tag{15}$$

where we consider for symmetry only $\xi > 0$ as before.

In Fig. 7, $P_y(\sigma)$ for the three different noise PDF's are shown for the intermediate amplitude $A = 0.2$, together with theoretical estimate $A_y(\sigma)$. As we anticipated, the performance of the disjoint uniform PDF exceeds all the others. In the small noise region ($L/2 < A$), our model (15) cannot reproduce the digital data due to the independence of our estimate from the shape of the periodic signal. As a peculiar feature of $P_{yd}(\sigma)$, a new maximum appears for large noise intensity, due to the superposition of the two uniform PDF's in the region $(b/2-A, b/2+A)$, correctly reproduced by (15).

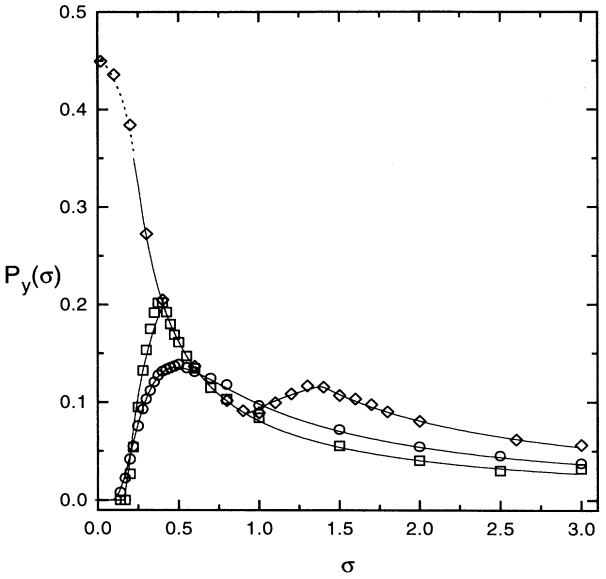

FIG. 7. P_y vs σ for Gaussian noise (circles), uniform noise (squares), and disjoint uniform noise (diamonds), $A = 0.2$. Theoretical predictions A_y are shown with solid lines, $k = 0.7$ as in Fig. 5. Statistical errors are within 10%. All the quantities are in a.u..

B. Multithreshold systems

Evidence of multipeaked curves has been recently reported [21] in the study of brain neurons triggered by external stimuli. It has been suggested that such a behavior could be addressed by physical models characterized by the presence of more than two stable states and thus by multithreshold systems. Without entering here into a detailed discussion of the many different models proposed, we consider the general features of our system (8) when we are not limited by three states (two thresholds) any more. Specifically, we consider the following system:

$$y(t) = \begin{cases} -n & \text{for } -\frac{(2n+1)}{2} < x < -\frac{(2n-1)}{2} \\ \vdots & \\ 0 & \text{for } -\frac{1}{2} < x < \frac{1}{2} \\ \vdots & \\ n & \text{for } \frac{(2n-1)}{2} < x < \frac{(2n+1)}{2} . \end{cases} \tag{16}$$

For a given n, we have $2n+1$ levels and $2n$ thresholds to cross. In Figs. 8 and 9, we show $P_y(\sigma)$ for the Gaussian

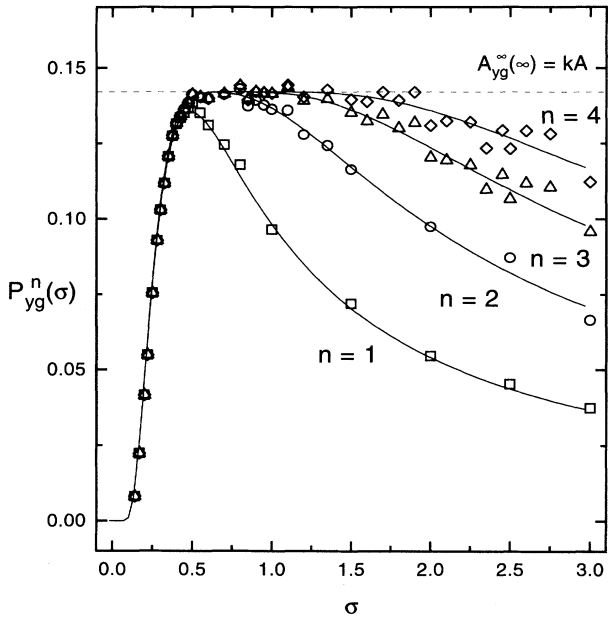

FIG. 8. P^n_{yg} vs σ with Gaussian noise for $n = 1$ (squares), $n = 2$ (circles), $n = 3$ (triangles), and $n = 4$ (diamonds). $A = 0.2$. Theoretical predictions A^n_{yg} are shown with solid lines, $k = 0.7$ as in Fig. 5. Statistical errors are within 10%. All the quantities are in a.u..

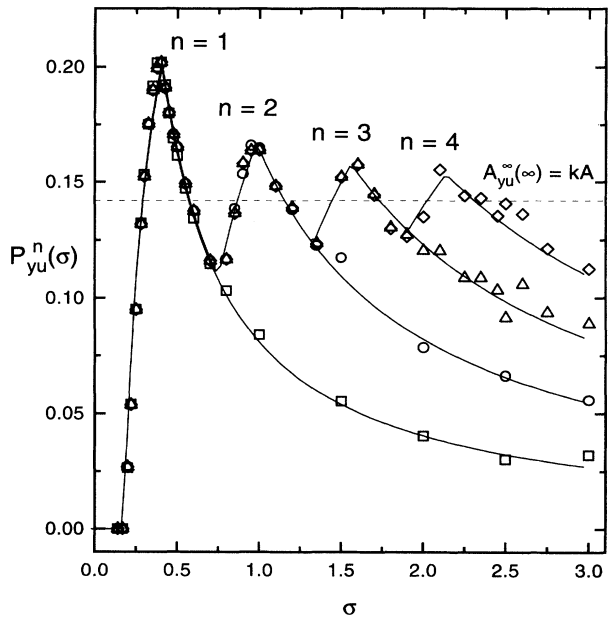

FIG. 9. P^n_{yn} vs σ with uniform noise for $n = 1$ (squares), $n = 2$ (circles), $n = 3$ (triangles), and $n = 4$ (diamonds). $A = 0.2$. Theoretical predictions A^n_{yu} are shown with solid lines, $k = 0.7$ as in Fig. 5. Statistical errors are within 10%. All the quantities are in a.u.

and uniform noise cases, respectively. In both cases, we experimentally explore $n = 1, 2, 3, 4$. The main features can be summarized as follows.

(a) $P^n_y(\sigma)$ vs σ behavior is common to all the $n > m$ curves up to a $\sigma \approx (2m+1)b/2$ value. For larger σ, higher n are explored and new thresholds come into play.

(b) In the Gaussian case, for finite n, $P^n_y(\sigma)$ shows a single maximum, in analogy with the $n = 1$ case. The bell shaped curve tends to become wider and smoother as n increases. When $n \to \infty$, the maximum disappears and the curve, for large σ, is characterized by a horizontal asymptote with value $P^{\infty}_y(\infty)$ (dotted line in Fig. 8).

(c) In the uniform noise case, $P^n_y(\sigma)$ presents n distinct maxima, in correspondence with $L = L_{\max}$ [$L_{\max} = (2m-1)b/2 + A$ for $m = 1, \ldots, n$], decreasing in amplitude. When $n \to \infty$, for large L, the curve oscillates around the asymptotic value $P^{\infty}_y(\infty)$ (dotted line in Fig. 9).

A theoretical description for system (16), with $n > 1$, follows from a generalization of the results already obtained for the simple case of $n = 1$. In this case we consider n distinct PDF area sectors, each separated by a distance equal to the threshold b. All the contributions, for increasing n, are added to give the quantity $A^n_y(\sigma)$:

$$A^n_y(\sigma) = \sum_{m=1}^{n} \left\{ F\left[\left(\frac{(2m-1)}{2}b + A\right)/\sigma\right] - F\left[\left(\frac{2m-1}{2}b - A\right)/\sigma\right] \right\} . \tag{17}$$

For the Gaussian case we have

$$A^n_{yg}(\sigma) = k \sum_{m=1}^{n} \left\{ \Phi\left[\left(\frac{(2m-1)}{2}b + A\right)/\sigma\right] - \Phi\left[\left(\frac{2m-1}{2}b - A\right)/\sigma\right] \right\} \tag{18}$$

and for the uniform case we have

$$A^n_{yu}(L) = B^n_{yu}(L) + C^n_{yu}(L)$$

with

$$B^n_{yu}(L) = k \sum_{m=1}^{n} \begin{cases} 0 & \text{for } \frac{L}{2} < \frac{b}{2} - A \\ \frac{1}{L}\left(\frac{L}{2} - \frac{(2m-1)}{2}b + A\right) + \frac{2A}{L}(m-1) & \text{for } \frac{2m-1}{2}b - A \le \frac{L}{2} \le \frac{2m-1}{2}b + A \\ \frac{2A}{L}m & \text{for } \frac{2m-1}{2}b + A \le \frac{L}{2} \le \frac{2m+1}{2}b - A \end{cases}$$

and

$$C_{yu}^{n}(L) = \frac{2A}{L}n \text{ for } \frac{L}{2} > \frac{2m+1}{2}b - A$$

in good agreement with digital data. The horizontal asymptote yields to $A_y^{\infty}(\infty) = A$ (see Figs. 8 and 9).

IV. CONCLUSIONS

The use of the word "resonance" for the SR phenomenon has been questioned since the very beginning [1]. Recently, it has been demonstrated [22] that, for a diffusion process, in a double well system, the meaning of "resonance" as the matching of two characteristic frequencies (or physical time scales) is indeed appropriate for such a phenomenon, if the residence time of the two states (in the bistable case) is taken into account as the order parameter. For this system, the resonant condition can be obtained either by changing the noise intensity or by changing the input signal frequency. For the threshold systems that we consider here, instead, such a frequency matching condition does not hold anymore [23] at the moment that we have only one characteristic frequency (periodic forcing). As expected, the change of the input frequency does not produce any effect on $P_y(\sigma)$ [20]. For this reason the output signal enhancement [24] typical of the SR phenomenon can be obtained, here, for nonperiodic signals as well.

It seems reasonable to conclude that SR in the threshold systems considered here, far from being a resonant phenomenon, can be more correctly interpreted as a special case of the dithering effect [6,25] consisting of a threshold crossing process aided by noise. For this class of effects the name "noise induced threshold crossings" seems more appropriate.

ACKNOWLEDGMENTS

The author would like to acknowledge F. Marchesoni and A.R. Bulsara for useful discussions and J. Kovalik for a careful reading of the manuscript.

[1] R. Benzi, G. Parisi, A. Sutera, and A. Vulpiani, Tellus **34**, 10 (1982); L. Gammaitoni, F. Marchesoni, E. Menichella-Saetta, and S. Santucci, Phys. Rev. Lett. **62**, 349 (1989); B. McNamara and K. Wiesenfeld, Phys. Rev. A **39**, 4854 (1989); P. Jung and P. Hänggi, Europhys. Lett. **8**, 505 (1989); G. Hu, G. Nicolis, and C. Nicolis, Phys. Rev. A **42**, 2030 (1990); R. F. Fox and Y. Lu, Phys. Rev. E **48**, 3390 (1993); for a recent review on the subject of SR, see Nuovo Cimento D (to be published); See also the WWW server on SR at *www.pg.infn.it/sr/*

[2] S. Fauve and F. Heslot, Phys. Lett. **97A**, 5 (1983); B. McNamara, K. Wiesenfeld, and R. Roy, Phys. Rev. Lett. **60**, 2626 (1988); L. Gammaitoni, E. Menichella-Saetta, S. Santucci, F. Marchesoni, and C. Presilla, Phys. Rev. A **40**, 2114 (1989); L. Gammaitoni, M. Martinelli, L. Pardi, and S. Santucci, Phys. Rev. Lett. **67**, 1799 (1991); J. Douglass, L. Wilkens, E. Pantazelou, and F. Moss, Nature **365**, 337 (1993); A. Simon, and A. Libchaber, Phys. Rev. Lett. **68**, 3375 (1992); R.N. Mantegna and B. Spagnolo, Phys. Rev. E **49**, R1792 (1994); R. Bartussek, P. Hanngi, and P. Jung, *ibid.* **49**, 3930 (1994).

[3] V.I. Melnikov, Phys. Rev. E **48**, 2481 (1993).

[4] P. Jung, Phys. Rev. E **50**, 2513 (1994); Nuovo Cimento D (to be published).

[5] Z. Gingl, L.B. Kiss, and F. Moss, Europhys. Lett. **29**, 191 (1995).

[6] T.R. Albert, A.R. Bulsara, G. Schmera, and M. Inchiosa (unpublished).

[7] A. V. Oppenheim and R.W. Schaffer, Digital Signal Processing, Prentice Hall Int., 1975.

[8] W.R. Bennet, Bell Syst. Technol. J. **27**, 446 (1948).

[9] L. Schuchman, IEEE Trans. Commun. Technol. **COM-12**, 162 (1964).

[10] B. Widrow, Trans. AIEE **79**, 555 (1960).

[11] L.G. Roberts, IRE Trans. Inf. Theor. **8**, 145 (1962)

[12] W.M. Goodall, Bell Syst. Technol. J. **30**, 33 (1951).

[13] D.J. Connor, R.C. Brainard, and J.O. Limb, Proc IEEE **60**, 779 (1972).

[14] J. Vanderkooy and S. Lipshitz, J. Audio Emg. Soc. **32**, 106 (1984).

[15] J.F. Blinn, IEEE Comput. Graph. Appl., **14**, 78 (1994).

[16] P. Carbone and D. Petri, IEEE Trans. Instr. Meas. **43**, 389 (1994).

[17] Here and in the following we consider noise sources with a power spectral density flat up to a cutoff frequency $\bar{\omega}$. The standard deviation σ is used as a measure of the noise intensity.

[18] J.P. Segundo, J.F. Vibert, K. Pakdaman, M. Stiber, and O. Diez Martinez, in *Proceedings of the Second Appalachian Conference*, edited by K. Pribram (IEEE Society Press, Los Alamitos, CA, 1994); M.F. Wagdy and M. Goff, IEEE Trans. Instr. Meas. **43**, 146 (1994); M.I. Dykman, D.G. Luchinsky, R. Mannella, P.V.E. McClintock, H.E. Short, N.D. Stein, and N.G. Stocks, Phys. Lett. A **193**, 61 (1994); M. Morillo and J. Gomez-Ordonez, Phys. Rev. E **51**, 999 (1995); M. Inchiosa and A. Bulsara, *ibid.* **52**, 327 (1995).

[19] M. Hauser, J. Audio Eng. Soc. **39**, 3 (1991).

[20] With $\omega_0 \ll \bar{\omega}$.

[21] E. Kaplan (private communication).

[22] L. Gammaitoni, F. Marchesoni, and S. Santucci, Phys. Rev. Lett. **74**, 1052 (1995).

[23] L. Gammaitoni, F. Marchesoni, E. Menichella-Saetta, and S. Santucci, Phys. Rev. Lett. **71**, 3625 (1993).

[24] The same effect is present also in the signal-to-noise ratio and it will be discussed in a forthcoming paper.

[25] K. Wiesenfeld and F. Moss, Nature **373**, 33 (1995).

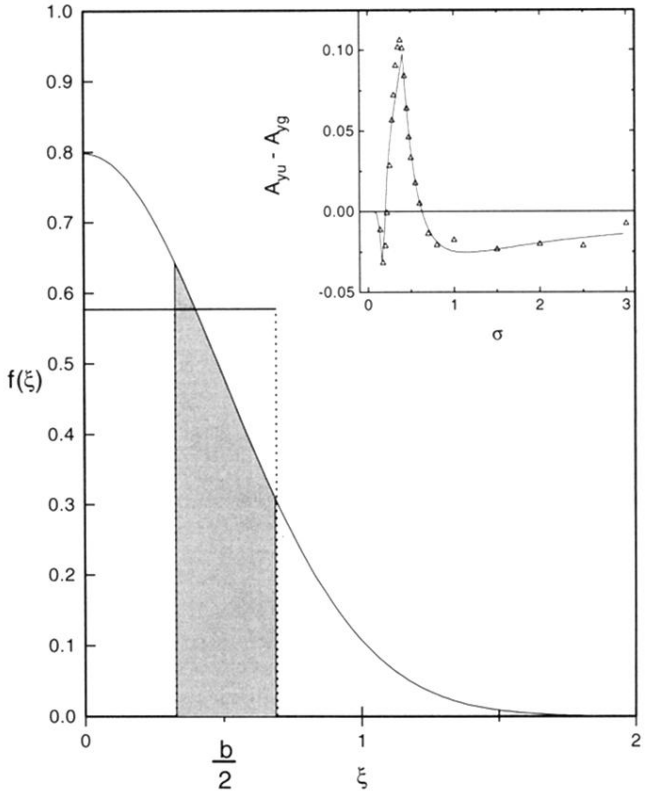

FIG. 6. $f(\xi)$ (a.u.) for Gaussian and uniform noise. The area under the distributions and enclosed between $b/2 - A$ and $b/2 + A$ (dotted lines) equals A_{yu} and A_{yg} (shaded area), $\sigma_g = \sigma_u = 1$ (a.u.). Inset: $A_{yu} - A_{yg}$ vs σ, $A = 0.2$ (a.u.), theroretical prediction (solid line), and experimental data $P_{yu} - P_{yg}$ (triangles).